Circulation Research

ORIGINAL RESEARCH

Sbk2, a Newly Discovered Atrium-Enriched Regulator of Sarcomere Integrity

Pim R.R. van Gorp, Juan Zhang, Jia Liu, Roula Tsonaka, Hailiang Mei, Sven O. Dekker, Cindy I. Bart, Tim De Coster, Harm Post, Albert J.R. Heck, Martin J. Schalij, Douwe E. Atsma, Daniël A. Pijnappels, Antoine A.F. de Vries

BACKGROUND: Heart development relies on tight spatiotemporal control of cardiac gene expression. Genes involved in this intricate process have been identified using animals and pluripotent stem cell-based models of cardio(myo)genesis. Recently, the repertoire of cardiomyocyte differentiation models has been expanded with iAM-1, a monoclonal line of conditionally immortalized neonatal rat atrial myocytes (NRAMs), which allows toggling between proliferative and differentiated (ie, excitable and contractile) phenotypes in a synchronized and homogenous manner.

METHODS: In this study, the unique properties of conditionally immortalized NRAMs (iAMs) were exploited to identify and characterize (lowly expressed) genes with an as-of-yet uncharacterized role in cardiomyocyte differentiation.

RESULTS: Transcriptome analysis of iAM-1 cells at different stages during one cycle of differentiation and subsequent dedifferentiation identified ≈13 000 transcripts, of which the dynamic changes in expression upon cardiomyogenic differentiation mostly opposed those during dedifferentiation. Among the genes whose expression increased during differentiation and decreased during dedifferentiation were many with known (lineage-specific) functions in cardiac muscle formation. Filtering for cardiac-enriched low-abundance transcripts, identified multiple genes with an uncharacterized role during cardio(myo) genesis including Sbk2 (SH3 domain binding kinase family member 2). Sbk2 encodes an evolutionarily conserved putative serine/threonine protein kinase, whose expression is strongly up- and downregulated during iAM-1 cell differentiation and dedifferentiation, respectively. In neonatal and adult rats, the protein is muscle-specific, highly atrium-enriched, and localized around the A-band of cardiac sarcomeres. Knockdown of Sbk2 expression caused loss of sarcomeric organization in NRAMs, iAMs and their human counterparts, consistent with a decrease in sarcomeric gene expression as evinced by transcriptome and proteome analyses. Interestingly, co-immunoprecipitation using Sbk2 as bait identified possible interaction partners with diverse cellular functions (translation, intracellular trafficking, cytoskeletal organization, chromatin modification, sarcomere formation).

CONCLUSIONS: iAM-1 cells are a relevant and suitable model to identify (lowly expressed) genes with a hitherto unidentified role in cardiomyocyte differentiation as exemplified by Sbk2: a regulator of atrial sarcomerogenesis.

GRAPHIC ABSTRACT: A graphic abstract is available for this article.

Key Words: cell line ■ myocytes, cardiac ■ protein kinases ■ sarcomeres ■ sequence analysis, RNA

In This Issue, see p 1 | Meet the First Author, see p 2

Formation of the 4-chambered mammalian heart is a complex process, orchestrated by tightly regulated expression in time, space, and amount of transcription factors as well as regulatory RNA molecules, which are often highly conserved between vertebrates and invertebrates.[1–3] Dysregulation of cardiac gene expression is associated with various types of congenital heart disease and with myocardial malfunction.[1,2] In the past, studies on the role of individual genes in heart development, cardiac cell differentiation, and cardiomyocyte function were mainly performed in (non)transgenic animal models like mouse, chicken, clawed frog, zebrafish, and fruit

Correspondence to: Antoine A.F. de Vries, PhD, Laboratory of Experimental Cardiology, Department of Cardiology, Leiden University Medical Center, Albinusdreef 2, 2333 ZA Leiden, the Netherlands. Email a.a.f.de_vries@lumc.nl
Supplemental Material is available at https://www.ahajournals.org/doi/suppl/10.1161/CIRCRESAHA.121.319300.
For Sources of Funding and Disclosures, see page 40.

Circulation Research is available at www.ahajournals.org/journal/res

Novelty and Significance

What Is Known?

- The formation and maintenance of heart muscle cells is a complex process regulated by multiple signal transduction pathways.
- Protein kinases are important effectors of signal transduction pathways involved in cardiomyocyte differentiation, homeostasis, and adaptation to environmental changes.
- Whole transcriptome analysis of heart muscle cells at different stages of cardiomyogenic differentiation is a powerful means to identify (cell type-specific) factors involved in cardiomyocyte formation.

What New Information Does This Article Contribute?

- Conditionally immortalized atrial cardiomyocytes are a novel, easy-to-use in vitro model to identify and characterize new factors involved in (atrial) cardiomyogenesis.
- Sbk2 (SH3 domain binding kinase family member 2) is a highly atrium-enriched protein localized near the A-band of cardiac sarcomeres.
- Knockdown of Sbk2 expression in atrial cardiomyocytes causes large changes in the gene expression profile of these cells at both the RNA and protein level and results in loss of well-structured sarcomeres indicating an important role of this gene in (atrial) cardiomyogenesis.

Little is known about the signal transduction pathways controlling atrial cardiomyocyte proliferation, (de)differentiation, and function. In this study, we exploited the unique ability of conditionally immortalized atrial cardiomyocytes to switch between proliferative (noncontractile) and differentiated (contractile) phenotypes to identify new regulators of atrial myogenesis. Transcriptome analysis of these atrial cardiomyocytes at different stages of the phenotypic conversion identified a large number of genes showing a strong increase in expression during cardiomyogenic differentiation followed by a large decrease in expression after subsequent dedifferentiation to a proliferative state. Among these were many genes with an as of yet unknown role in cardiomyocytes including Sbk2, which encodes a serine/threonine-protein kinase. We found Sbk2 to be preferentially expressed in atrial cardiomyocytes with the protein being localized in close vicinity to the sarcomeric A-band. Knockdown of Sbk2 caused dramatic changes in the gene expression profile of these cells at both the mRNA and protein level and disturbed sarcomerogenesis. Pull-down assays using Sbk2 as bait identified possible interaction partners with functions in translation, intracellular trafficking, cytoskeletal organization, and sarcomere formation. Thus, conditionally immortalized atrial cardiomyocytes are a relevant and suitable model to identify genes with a hitherto unidentified role in cardiomyocyte differentiation as exemplified by Sbk2: a regulator of atrial sarcomerogenesis.

Nonstandard Abbreviations and Acronyms

(i)PSCs	(induced) pluripotent stem cells
Actc1	cardiac α-actin
Actn2	cardiac α-actinin
AMs	atrial myocytes
CDKs	cyclin-dependent kinases
eGFP	enhanced green fluorescent protein
GO	gene ontology
GSKs	glycogen synthase kinases
HA~RnSbk2	epitope-tagged RnSbk2
HA~βGal	epitope-tagged *Escherichia coli* β-galactosidase
hiAMs	conditionally immortalized human AMs
HsSBK2	human SBK2
iAMs	conditionally immortalized NRAMs
LVV	lentiviral vector
MAPKs	mitogen-activated protein kinases
Mki67	proliferation marker Ki-67
MLC2a	atrial regulatory myosin light chain
MLC2v	ventricular regulatory myosin light chain
Mybpc3	cardiac myosin-binding protein C
MyHC	myosin II heavy chain
NKF1	new kinase family 1
NRAMs	neonatal rat atrial myocytes
Ppluc	firefly luciferase
RNA-Seq	RNA sequencing
RnNkx2-5	rat Nkx2-5
RnSbk2	rat Sbk2
RT-qPCR	reverse transcription-quantitative polymerase chain reaction
Sbk2	SH3 domain binding kinase family member 2
shRNAs	short hairpin RNAs
Tnni3	cardiac troponin I

fly.[4–7] These studies have benefited greatly from recent advances in transcriptome analysis using next-generation RNA sequencing (RNA-Seq) techniques. This allowed assessment of the dynamic changes in the expression of individual genes even at the single-cell level and discrimination of different cellular phenotypes on the basis of distinct gene expression profiles.[8] Despite the knowledge acquired from (transgenic) animal models, their current extensive use is subject to an ongoing ethical debate and limited within strict boundaries enforced by animal welfare committees.[9]

Recently, (induced) pluripotent stem cells ([i]PSCs) have been introduced as alternative models to study cardiac development and differentiation. These in vitro models not only recapitulate many of the features of cardio(myo)genesis observed in animal models but also allow a more detailed analysis of certain aspects of the process due to the relative ease with which they can be handled and manipulated.[3,10] Furthermore, (i)PSCs can be differentiated into different kinds of cardiomyocytes (eg, atrial, nodal, and ventricular cardiomyocytes) facilitating the detailed characterization of individual cardiomyocyte types.[11] Despite the advantages of (i)PSC-based models of cardio(myo)genesis, their application is currently limited by several factors: (1) Derivation of cardiomyocytes from (i)PSCs is a complex and intensive process with a variable outcome. (2) Producing large numbers of cardiomyocytes with a high degree of phenotypic uniformity from (i)PSCs is difficult and expensive, requiring special selection and sorting methods. (3) (i)PSC-derived cardiomyocytes typically have an immature phenotype and are thus structurally and functionally different from adult cardiomyocytes.[12,13]

While next-generation RNA-Seq methods have yielded a wealth of information about the cardiac developmental changes in the expression of genes showing moderate to high transcriptional activity, studying the dynamics of low-abundance transcripts (eg, minor splice variants) during cardio(myo)genesis is still challenging.[14–16] In most cases, low-abundance transcripts are excluded during differential expression analysis, which can at least be partially overcome by an increase in sequencing depth and the application of various cell and RNA enrichment procedures.[17–20] The use of relatively homogenous cell populations as starting material can also simplify the analysis of the developmental changes in the transcription of lowly expressed genes. Our research group recently published a line of conditionally immortalized neonatal rat atrial myocytes (NRAMs), called iAM-1.[21] Culturing of iAM-1 cells in the presence of doxycycline triggers cell division, while in doxycycline-free culture medium, these cells spontaneously and synchronously differentiate into fully functional (ie, excitable and contractile) atrial myocytes (AMs). This unique property makes inducible AMs (iAMs) an attractive alternative model to investigate the role of especially lowly expressed genes in cardiomyocyte proliferation and differentiation.

In this study, RNA-Seq was performed on samples harvested at various time points during a full cycle of iAM-1 cell differentiation and subsequent dedifferentiation. For most genes, the dynamic changes in expression during cardiomyogenic differentiation opposed those observed during dedifferentiation. Differential expression analysis, a quasi-Poisson regression model and filtering for genes preferentially expressed in rat hearts were used to identify low-abundance transcripts with an unknown role during cardiomyocyte differentiation or dedifferentiation. This resulted in the identification of multiple genes with an uncharacterized role during cardio(myo)genesis, among which Sbk2 (SH3 domain binding kinase family member 2, also known as Sgk069). Sbk2 codes for a serine/threonine-protein kinase, whose amino acid sequence is highly conserved among coelomates. Expression of Sbk2 is upregulated during iAM-1 cell differentiation and downregulated during the subsequent return to a proliferative phenotype. Database searching, reverse transcription-quantitative polymerase chain reaction (RT-qPCR) analysis, Western blotting, and immunostaining of histological sections and cultured cells showed that the Sbk2 protein is highly enriched in atrial cardiomyocytes and localized around the myosin heads of cardiac sarcomeres. Lentiviral knockdown revealed a role for rat Sbk2 (RnSbk2) and human SBK2 (HsSBK2) in maintaining sarcomeric integrity. Sbk2 up- or downregulation did, however, not affect the electrophysiological properties of cardiomyogenically differentiated iAMs in confluent monolayer cultures as assessed by optical voltage mapping. Analysis of the molecular consequences of Sbk2 knockdown in differentiated iAM-1 cells by RNA-Seq and mass spectrometry implicated Sbk2 as an important regulator of a variety of cellular processes including sarcomerogenesis. In line with these findings, co-immunoprecipitation using lysates of differentiated iAM-1 cells identified proteins with diverse cellular functions (translation, intracellular trafficking, cytoskeletal organization, chromatin modification, sarcomere formation) as possible interaction partners of Sbk2.

METHODS

Data Availability

Extended Methods are available in the Supplemental Material. The iAM-1 RNA-Seq data have been deposited in the Gene Expression Omnibus (GSE164763 and GSE186626). For a complete list of the research materials, see the Major Resources Table in the Supplemental Material.

Animal Experiments

Animal experiments were approved by the Leiden University Medical Center Animal Experiments Committee and conformed to the Guide for the Care and Use of Laboratory Animals as stated by the US National Institutes of Health.

Culture of Primary Neonatal Rat Cardiomyocytes and of Conditionally Immortalized AMs of Rat and Human

The isolation and culture of neonatal rat cardiomyocytes as well as the generation and culture of conditionally immortalized AMs of rat and human were done essentially as described previously.[21,22]

RNA and Protein Analyses

The extraction of total RNA and protein from tissue and cells are described in the Extended Methods in the Supplemental Material. The primer pairs used to quantify the relative expression of RnSbk2 and of HsSBK2 by RT-qPCR are listed in Table S4. Western blot analysis was performed as described before using the primary and secondary antibodies presented in Tables S2 and S3.[21]

RNA-Seq

RNA-Seq was performed on an Illumina HiSeq 4000 or NovaSeq 6000 Sequencing System. FASTQ files were processed, aligned to the rat reference genome Rnor_6.0 and normalized for sequencing depth (counts per million) or mRNA length (transcripts per million). Differential gene expression analysis was performed using the edgeR Bioconductor[23] (version 3.26.8) or DESeq2[24] (version 2-1.14). In the edgeR Bioconductor, differentially expressed genes were identified by a quasi-Poisson regression model and genes of cardiac relevance were selected using the rat RNA-Seq transcriptomic BodyMap.[25] The Gene ontology (GO) annotation enrichment analysis was performed using DAVID Bioinformatics Resources (version 6.8), and the top biological process categories with Benjamini-Hochberg-corrected *P* values <0.05 were reported.[26]

Construction of LVV Shuttle Plasmids and Generation of LVV Particles for RnSbk2/HsSBK2 Overexpression and Knockdown Studies

Maps of the transgenes used for the knockdown and overexpression experiments described in this study are presented in Figure S11. All these transgenes were incorporated into lentiviral vector (LVV) shuttle plasmids with a hybrid Rous sarcoma virus/HIV type 1 5′ long terminal repeat and a self-inactivating (ie, unique region 3-deleted) 3′ long terminal repeat. LVV particles were produced from these constructs using a previously published method.[21] The absence of mistakes in the short hairpin RNA (shRNA)- and protein-coding parts of the transgenes was confirmed by Sanger sequencing.

Immunostainings

Tissue and cells were processed for immunostaining as detailed in the Extended Methods in the Supplemental Material and incubated with the primary and secondary antibodies presented in Tables S2 and S3. Since the Sbk2- and Sbk3-specific antibodies used in this study have not been (extensively) characterized, their specificity was validated in dedicated Western blot experiments and by immunocytochemistry (Results in the Supplemental Material and Figure S12).

Statistical Analysis

Data were expressed as mean and corresponding SD, unless stated otherwise. RT-qPCR data are presented as mean relative quantities and their corresponding SD. The statistical analyses were performed in GraphPad Prism (version 8.4.2). Statistical significance was expressed by *P* values and considered statistically significant at *P* values <0.05.

RESULTS

iAMs as Model of Cardiomyocyte Differentiation, Dedifferentiation, and Proliferation

To realize a full cycle of differentiation and dedifferentiation for detailed characterization, proliferating iAM-1 cells were cultured for 9 days (d0–d9) in the absence of doxycycline and subsequently for 9 days (d9–d18) in its presence. At day 0, 1, 2, 3, 9, 10, 11, 12, and 18, cells were fixed for immunocytochemistry and total RNA was harvested for RNA-Seq (Figure 1A). As expected and consistent with previous results, most nuclei of d0 iAM-1 cells were strongly positive for the proliferation marker Ki-67 (Mki67), whereas in the cytoplasm of proliferating iAM-1 cells, a weak and uniform staining for the sarcomeric Z-line marker Actn2 (cardiac α-actinin) was observed (Figure 1B).[21] As reported before, removal of doxycycline triggered cardiomyogenic differentiation of the iAM-1 cells as evinced by a complete loss of the Mki67 signal within 2 days (Figure 1B).[21] In parallel, the cytoplasmic Actn2 signal gradually increased and evolved from a highly diffuse pattern into a more punctate distribution reflecting the formation of premyofibrils (Figure 1B, d3) and, finally, into the cross-striated pattern typical of mature myofibrils (Figure 1B, d9). The formation of mature myofibrils coincided with the appearance of synchronized and spontaneous contractions. Adding doxycycline to the fully differentiated iAM-1 cells, resulted in disassembly of the sarcomeres (Figure 1B, d10–d12) and a gradual decrease of Actn2 (Figure 1B, d9–d12). This dedifferentiation process was accompanied by the reappearance of Mki67$^+$ cells (Figure 1B, d11–d18) and the resumption of cell division causing a strong increase in cell density (Figure 1B, d12 and d18). Taken together, these findings demonstrate the ability of iAMs to switch between proliferative and differentiated states in a synchronized, doxycycline-dependent manner and validate the utility of these cells as model to study cardiomyocyte differentiation, dedifferentiation, and proliferation.

Transcriptome Dynamics During iAM-1 Cell Differentiation and Dedifferentiation

To investigate the changes in gene expression profile during the switch from a proliferative to a contractile phenotype and vice versa, samples collected at different time

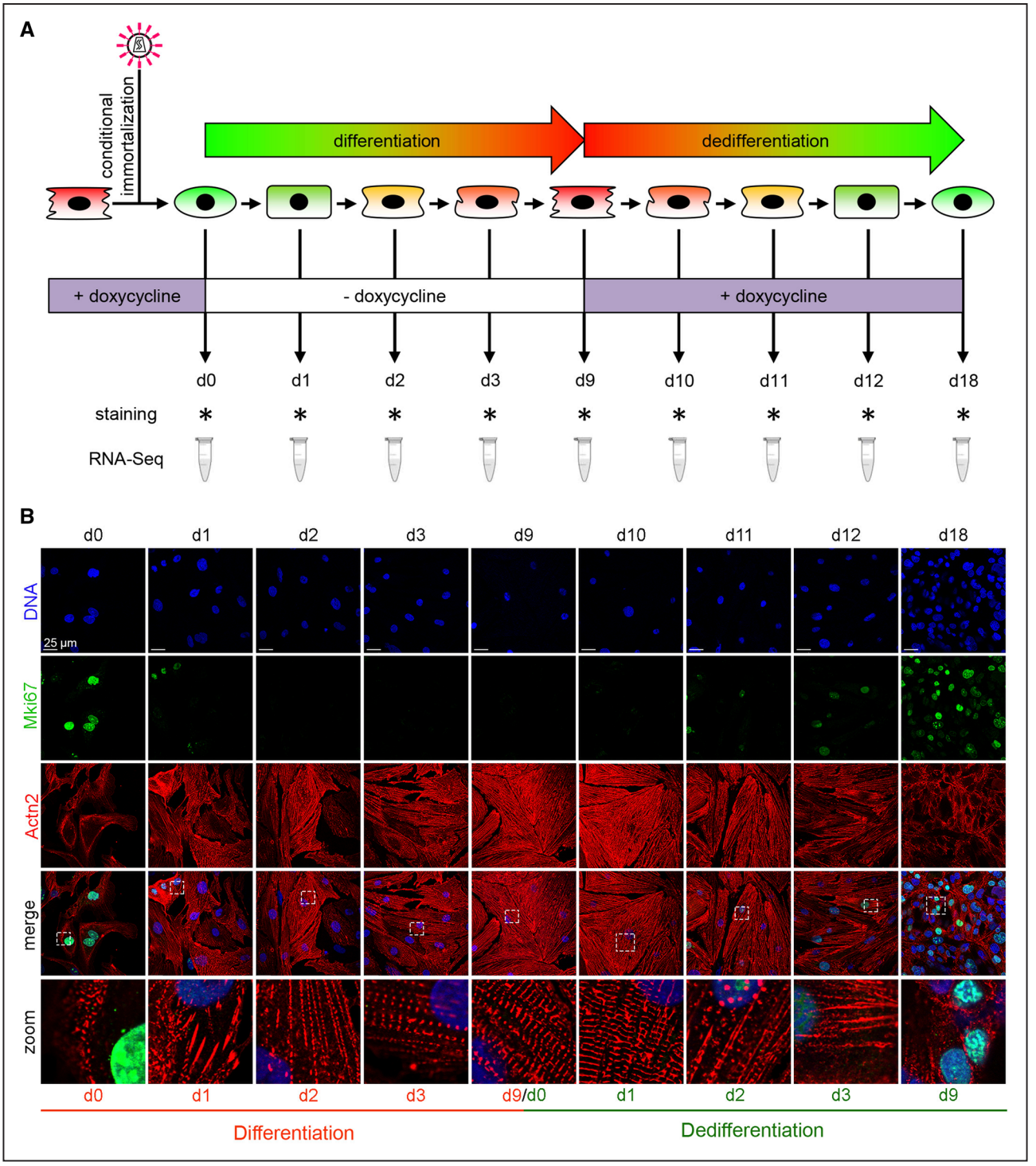

Figure 1. Conditionally immortalized neonatal rat atrial myocytes (iAMs) as a model of cardiomyocyte differentiation, dedifferentiation and proliferation.

A, Schematic overview of one round of iAM-1 cell differentiation (— doxycycline) and subsequent dedifferentiation (+ doxycycline). At the indicated days (d0–d18), cells were fixed for immunocytochemistry and snap-frozen for total RNA extraction. **B**, Immunocytological double staining of iAM-1 cells fixed at different stages of cardiac differentiation and dedifferentiation for the proliferation marker Ki-67 (Mki67; green) and for Actn2 (cardiac α-actinin; red). Cell nuclei are stained blue using the DNA-binding dye Hoechst 33342.

points during a complete cycle of iAM-1 cell differentiation and dedifferentiation were analyzed by RNA-Seq (Figure 1A; for transcript IDs and average count per million and transcripts per million values, see Table S5). This yielded the dendrogram (Figure S1A) of transcriptional relatedness between samples, which is further discussed in the Results in the Supplemental Material. Principle component analysis confirmed the similarity between

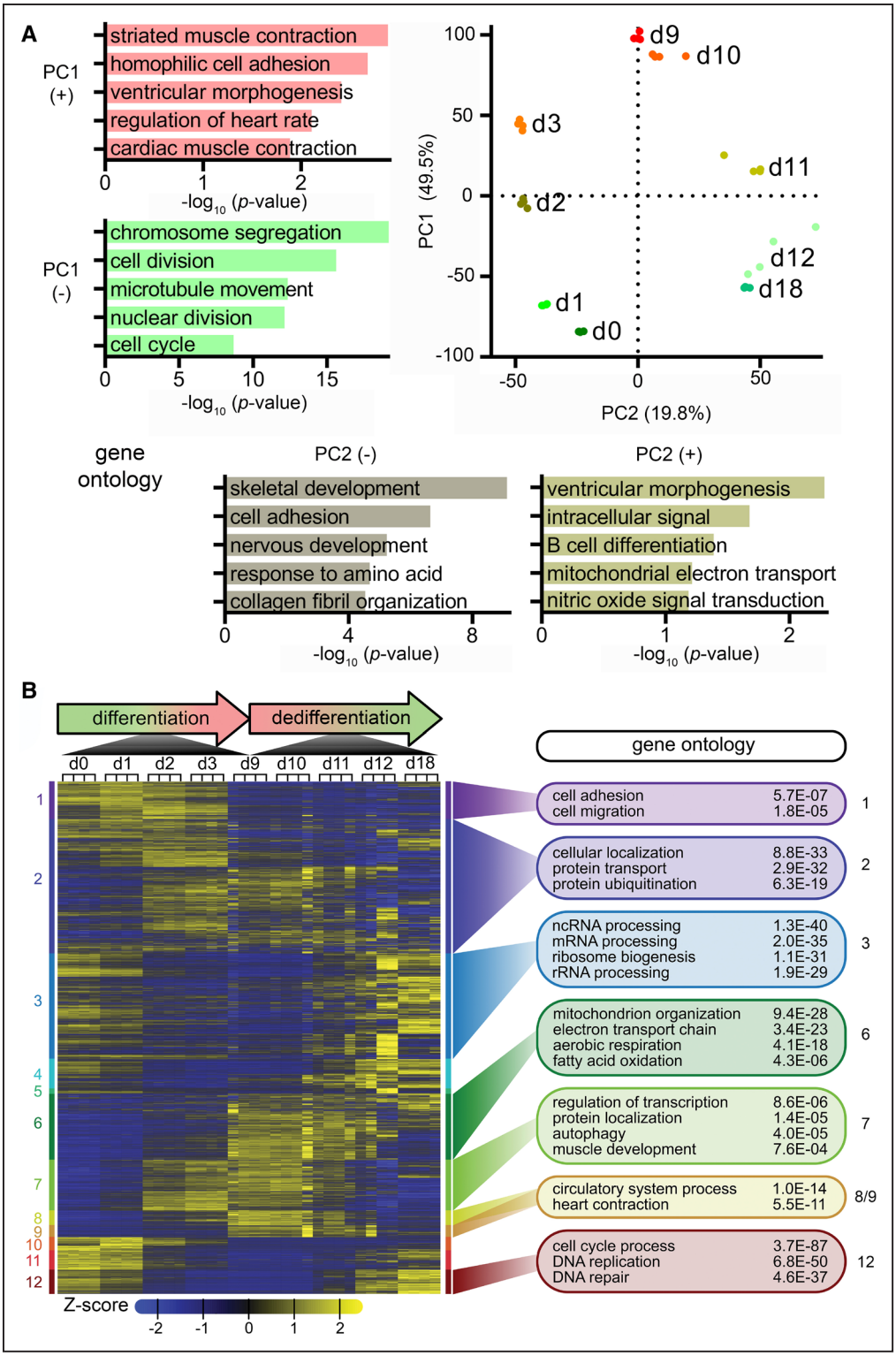

Figure 2. Transcriptome dynamics during conditionally immortalized neonatal rat atrial myocyte (iAM-1 cell) differentiation and dedifferentiation.

A, Principle component (PC) analysis of RNA-Seq data corresponding to one round of iAM-1 cell differentiation (d0–d9) and subsequent dedifferentiation (d9–d18). The different sampling time points (d0–d18, n=4) are represented by dots in a scatter plot of the PC1 (*y* axis) and PC2 (*x* axis) scores, corresponding to 49.5% and 19.8% of the variation in gene expression, respectively. The graphs at the **left** side and below the scatter plot show the result of a gene ontology (GO) annotation enrichment analysis of the top 100 genes in each of the 4 clusters. **B**, Heatmap showing the hierarchical clustering of global gene expression during iAM-1 cell differentiation (d0–d9) and subsequent dedifferentiation (d9–d18). The yellow and blue color codes are based on the calculated *Z* scores. For selected gene clusters, the assigned GO terms are shown, including their statistical significance as represented by the corrected *P* values (Benjamini-Hochberg method). For nonabbreviated GO terms, see Table S6.

samples taken at the same time point and showed that especially changes in principle component 1 (corresponding to 49.5% of variation) during differentiation (d0–d9; Figure 2A; Figure S1B and S1C; and Table S6) were mostly reversed during dedifferentiation (d9–d18). GO enrichment analysis of principle component 1 (Figure 2A) revealed that cardiomyogenic differentiation (d0–9) was accompanied by a switch from the expression of genes with a role in mitosis to the expression of genes involved in heart formation and muscle contraction, while the opposite took place during subsequent iAM-1 cell dedifferentiation (d9–d18). GO enrichment analysis of principle component 2 showed a similar trend with the upregulation of genes associated with cardiac muscle function during iAM-1 cell differentiation (Figure 2A). These observations are supported by heatmap analysis of the gene expression profiles grouped per sampling time point (Figure 2B; Table S6). Genes involved in DNA replication and cell cycle processes were gradually downregulated during cardiomyogenic differentiation (d0–d9, cluster 12, Figure 2B), while being upregulated again during iAM-1 cell dedifferentiation (d9–d18, cluster 12, Figure 2B). On the contrary, genes involved in circulatory system processes and heart contraction (cluster 8 and 9, Figure 2B) as well as in mitochondrion organization and activity including fatty acid oxidation (cluster 6, Figure 2B) were upregulated during differentiation of iAM-1 cells (d0–d9), while being downregulated again during their subsequent dedifferentiation (d9–d18). Overall, the RNA-Seq data are in line with the immunocytochemical staining results (Figure 1B), showing that in the absence of doxycycline, iAM-1 cells switch from a noncontractile proliferative phenotype to a nonproliferative contractile phenotype, which is mostly reversed following re-exposure to doxycycline.

Differentially Expressed Genes During iAM-1 Cell Differentiation and Dedifferentiation

For most genes, the heatmap of the iAM-1 transcriptome showed gradual and opposite changes in their Z-score during differentiation and dedifferentiation. Based on this observation and the longitudinal experimental design, we employed a quasi-Poisson regression model to fit changes in the levels of individual transcripts (n=12948) during iAM-1 cell differentiation (phase I) and dedifferentiation (phase II; Table S7).[27] Genes showing a significant ≥2-fold increase or decrease (ie, a slope ≥|0.077| and an adjusted *P* value <0.05) in transcriptional activity during differentiation and dedifferentiation were considered differentially expressed (Figure S2A and S2B). As expected, many of the differentially expressed genes that were downregulated during iAM-1 cell differentiation and upregulated during subsequent dedifferentiation are involved in cell proliferation, like Ccna2, Cdk2, Mki67, and Pole (Figure S2C). Conversely, differentially expressed genes whose expression increased during the differentiation of iAM-1 cells and decreased again during their dedifferentiation typically code for proteins with a specific functional role in cardiomyocytes. Examples of such genes include Nkx2-5 and Tbx5 encoding cardiac transcription factors, Scn5a and Kcnj5 specifying cardiac ion channels, Ryr2 and Casq2 encoding cardiomyocyte-specific Ca^{2+} handling proteins, Actn2 and Tnnt2 coding for cardiomyocyte-specific sarcomeric proteins and Atp5me and Mb encoding proteins important for cardiac ATP production (Figure S2D through S2H). Also upregulated in phase I and downregulated in phase II was the expression of the abundantly transcribed atrial marker genes Myl4 and Nppa (Figure S2I) as well as that of Myl7 and Sln. In contrast, ventricular marker genes were either not expressed in iAM-1 cells (eg, Irx1-6, Myl2) or were expressed at a (very) low and fairly constant level during iAM-1 cell differentiation (eg, Myl3) consistent with the atrial origin of the iAM-1 cell line. For additional information about the transcriptional differences between iAM-1 populations at the early stages of differentiation and dedifferentiation and between iAM-1 cells before the start of the differentiation process (d0) and at the end of the dedifferentiation process (d18), see Results in the Supplemental Material, Figure S3 and Table S8. Altogether, these results demonstrate that the quasi-Poisson regression model allows identification of genes with specific roles in cardiomyocyte differentiation (and function) or in cardiomyocyte proliferation.

Identification of Novel Low-Abundance Transcripts Upregulated During iAM-1 Cell Differentiation

In an attempt to identify genes with a so far uncharacterized role in (atrial) cardiomyocyte differentiation, the differentially expressed genes (n=4129, 31.9%) were organized in a Venn diagram based on the combined changes in gene expression during differentiation and dedifferentiation (Figure 3A; Table S7). GO enrichment analysis showed that genes only upregulated during cardiomyogenic differentiation (n=445, cluster a, Figure 3A) are involved in ATP metabolic processes and ion transmembrane transport, while genes only downregulated during phase I, are engaged in cell adhesion and cell migration (n=550, cluster d, Figure 3A). On the opposite, genes only upregulated during dedifferentiation (n=748, cluster b, Figure 3A) play a role in DNA replication and cell cycle processes, while genes only downregulated in phase II (n=685, cluster e, Figure 3A) are involved in receptor signaling and responses to chemical stimuli. Genes that are downregulated during cardiomyogenic differentiation and upregulated again during subsequent dedifferentiation (n=1013, cluster c, Figure 3A) play a role in, among others, organelle fission and mitotic cell cycle processes. In contrast, genes

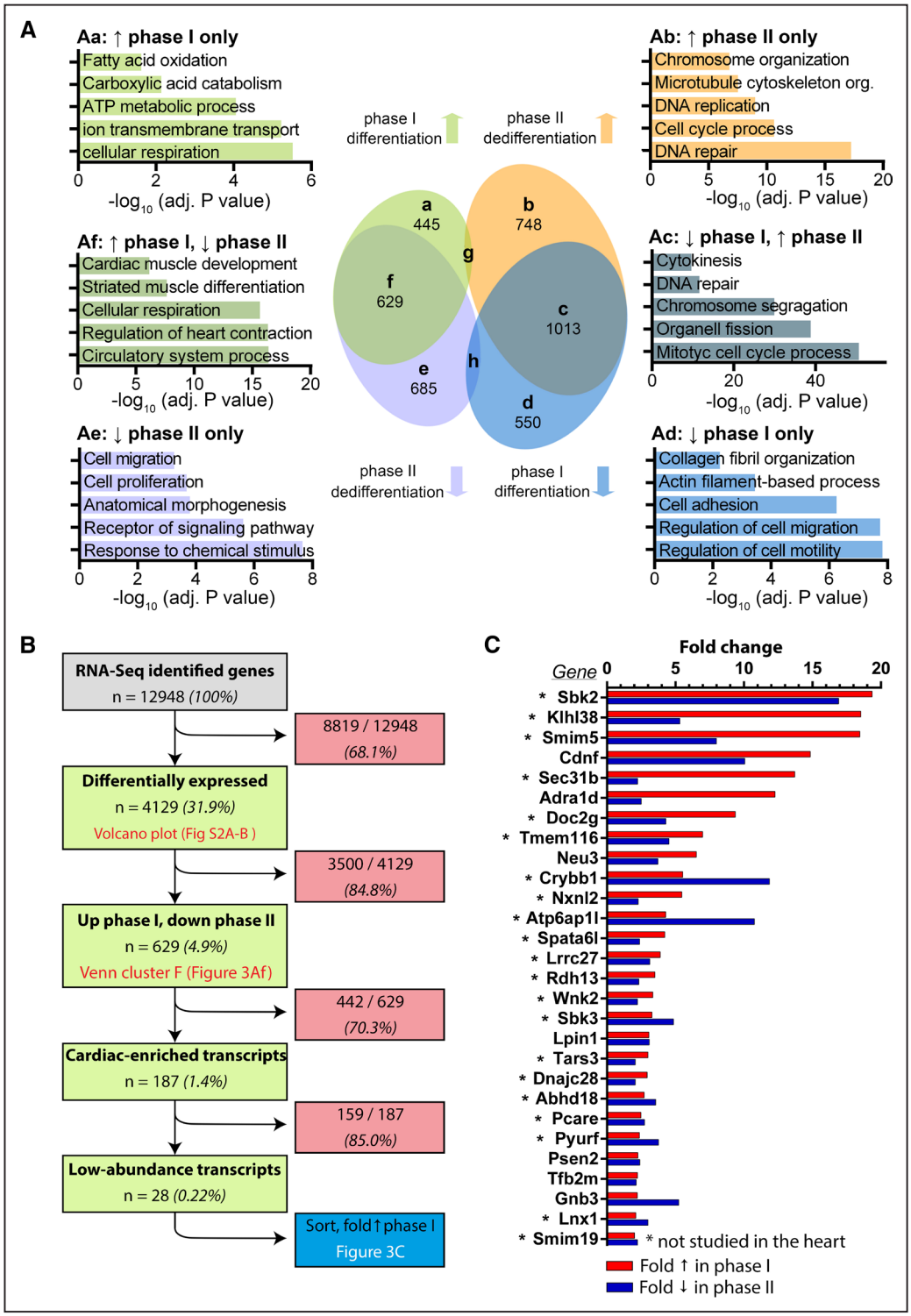

Figure 3. Differentially expressed genes during conditionally immortalized neonatal rat atrial myocyte (iAM-1 cell) differentiation and dedifferentiation.

A, Venn diagram of differentially expressed genes (≥2-fold change, adjusted [adj.] *P* value <0.05 [Benjamini-Hochberg method]) during iAM-1 cell differentiation (phase I) and subsequent dedifferentiation (phase II). The different clusters are indicated with the letters a-h. For each cluster, except clusters g and h, the number of differentially expressed genes and associated gene ontology (GO) terms are shown. For nonabbreviated GO terms, see Table S7. **B**, Schematic overview of the strategy to identify cardiac-enriched transcripts of low abundance with a potential role in the differentiation of atrial myocytes (AMs). **C**, Selected low-abundance transcripts sorted (from high to low) based on their fold increase during iAM-1 cell differentiation (red bars). For each gene, the fold decrease in expression level during subsequent iAM-1 cell dedifferentiation is also shown (blue bars). Genes that have not yet been studied in the context of the heart are marked with a star (*).

that are upregulated during phase I and downregulated again during phase II (n=629, cluster f, Figure 3A) are engaged in muscle development and differentiation as well as in heart contraction.

For the identification of uncharacterized genes with a potential role in cardio(myo)genesis, we focused on the genes in cluster f (Figure 3A) encoding cardiac-enriched transcripts based on the rat BodyMap database[25] (Figure 3B). Many of the genes (n=187, 1.4%) that remained after application of this filter are known for their striated or cardiac muscle-specific expression as exemplified by the presence of Myh6, Myh7, Myl4, Myl7, Myoz2, Nkx2-5, Nppa, Pln, Scn5a, Slc8a1, Sln, Smyd1, Tnnc1, Tnnt2, and Unc45b. Additional filtering was done by selecting the top 50 low-abundance and cardiac-enriched transcripts from the iAM-1 RNA-Seq and rat BodyMap databases (Table S7). The genes encoding the shared transcripts (n=28, 0.22%) were sorted based on the fold increase in their expression level during iAM-1 cell differentiation (Figure 3C). Three-quarters of these genes appeared not to have been studied in the context of the heart before (marked by *). Since, of all uninvestigated genes, Sbk2 showed the highest fold increase (ie, 19.4-fold, adjusted *P* value <0.005) during iAM-1 cell differentiation and a similarly large decrease (ie, 16.9-fold, adjusted *P* value <0.01) during subsequent dedifferentiation (Figure 3C), it was selected for functional characterization.

Sbk2 Is a Muscle-Specific, Atrium-Enriched Protein Associated With Sarcomeres

The Sbk2 gene of *Rattus norvegicus* (ENSRNOT 00000058956.3) is located in chromosome region 1q12 (Figure 4A), contains 4 exons similar to its human orthologue and codes for a single protein with a predicted molecular weight of 39.7 kDa. This presence of 4 exons and the precise location of the boundaries between exons and introns in the RnSbk2 gene are confirmed by the sashimi plot of RNA-Seq reads of differentiated (ie, d9) iAM-1 cells (Figure 4A). Although the overall expression of RnSbk2 is low (transcripts per million at d9 ≈25 as compared with ≈275 for Nkx2-5 and >20 000 for Myl4), it shows an exponential increase during iAM-1 cell differentiation followed by an exponential decrease during dedifferentiation (Figure 4B). A similarly strong differentiation-dependent increase of HsSBK2 expression was observed in a recently established atrial in vitro model consisting of conditionally immortalized human AMs (hiAMs) with preserved cardiomyogenic differentiation ability (Results in the Supplemental Material and Figure S4B through S4D).[22] RT-qPCR analysis of neonatal rat tissues revealed that Sbk2 is mainly expressed in muscle tissues with an up to 60-fold higher expression in atrial muscle than in ventricular or skeletal muscle, respectively (Figure 4D). These results are consistent with Western blot analyses showing the presence of a single protein species of ≈39 kDa in the atria, which was barely or not detectable in the other samples (Figure 4C). Multiple sequence alignment of the RnSbk2 amino acid sequence reveals a high degree of conservation among coelomates (Figure S5A and S5B). Furthermore, each of the 11 conserved amino acid domains identified in serine/threonine-protein kinases are retained in the aligned Sbk2 orthologues supporting an essential role of Sbk2 during coelomate evolution.[28]

Immunostaining of coronal heart sections from neonatal rats confirmed preferential expression of Sbk2 in the atria (Figure 4H and 4K), in contrast to the Z-line marker desmin, which is expressed at similar levels throughout the entire heart (Figure 4E and 4K). Sbk2 is undetectable in the aortic valves and aortic arch (Figure 4H, box) and only found in desmin-positive cells implying lack of expression in cardiac endothelial cells and fibroblasts (Figure 4I and 4 L). Investigation of the subcellular localization of Sbk2 by confocal fluorescence microscopy of the tissue sections, demonstrated that the protein surrounds desmin and hence may be associated with sarcomeric I- or A-bands (Figure 4J and 4M). In adult rats, a similar tissue distribution and subcellular localization was observed as shown by RT-qPCR, Western blotting and immunohistochemistry, respectively (Figure S6). Notably, myocardial expression of Sbk2 in adult rats appeared higher as compared with their neonatal counterparts (Figure S6C).

Sbk2 Is Localized Near the Myosin Heads in the Sarcomeric A-band of Neonatal and Adult Rat Hearts as well as Human Atrial Appendages

To further pinpoint the subcellular localization of RnSbk2, additional markers (ie, MLC2a [atrial regulatory myosin light chain], MLC2v [ventricular regulatory myosin light chain], MyHC [myosin II heavy chain] tail region, and Tnni3 [cardiac troponin I]) were used for co-localization studies in neonatal rat hearts (Figure 5A through 5 L). Sbk2 showed a clear co-localization with MLC2a (Figure 5A through 5C) as well as MLC2v (Figure 5D through 5F) and is (homogenously) expressed throughout the ventricular wall (Results in the Supplemental Material and Figure S7). Co-localization with the tail region of MyHC, which spans the sarcomeric A-band, was incomplete in both the atria and ventricles (Figure 5G through 5I) and showed the Sbk2 signal to be slightly more skewed towards the sarcomeric Z-line. Additionally, there was no clear co-localization of Sbk2 with Tnni3 (Figure 5J through 5 L), which spans both the sarcomeric I-band as well as a part of the A-band. Similar co-localization patterns between Sbk2 and the various sarcomeric markers were observed in the adult rat heart (Figure S8) as well as in human atrial appendages (Figure S9). Immunostaining

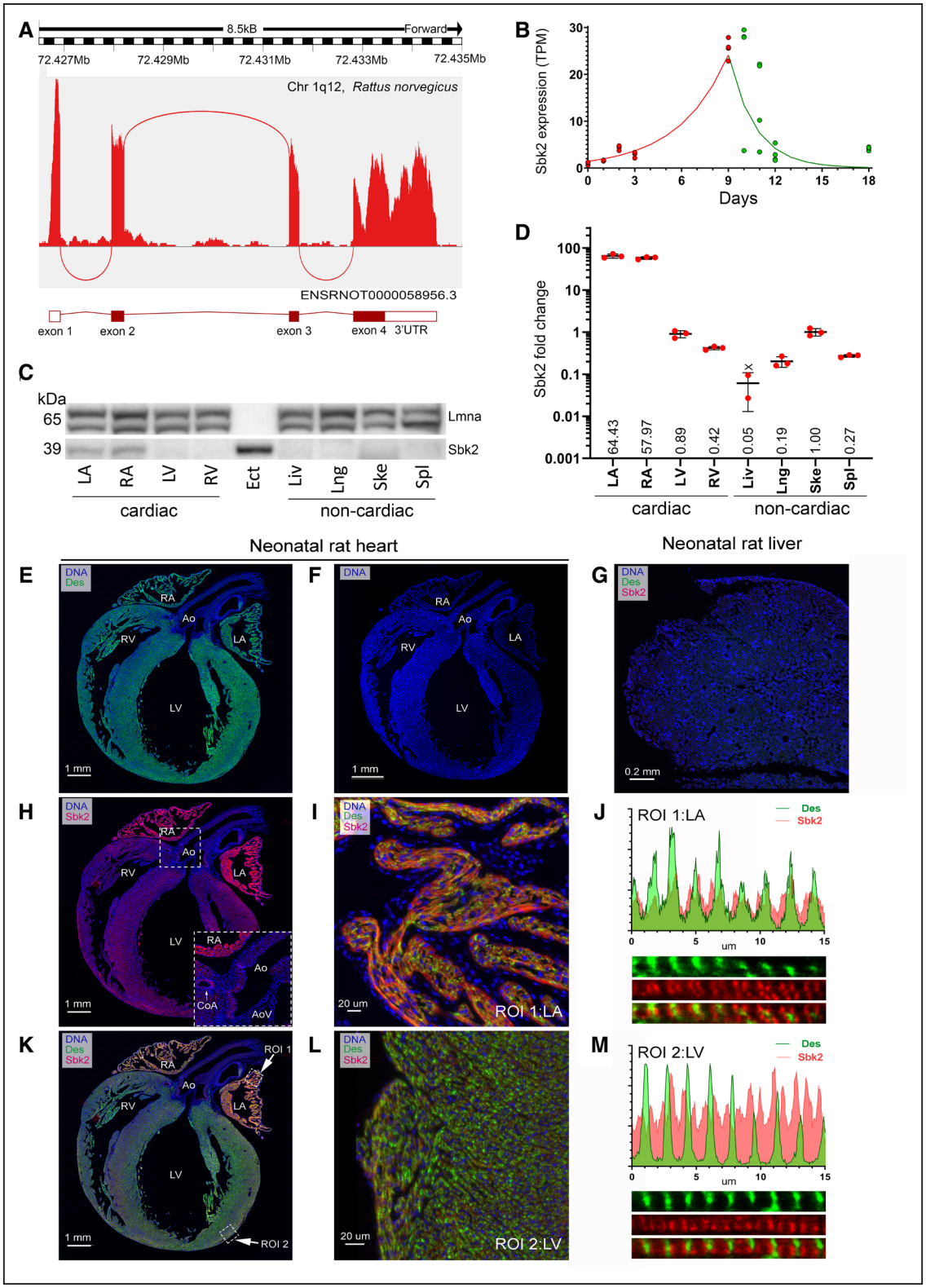

Figure 4. Sbk2 (SH3 domain binding kinase family member 2) is a muscle-specific, atrium-enriched protein associated with sarcomeres.

A, Sashimi plot of RNA-Seq reads of conditionally immortalized NRAMs (iAM-1 cells) at day 9 of differentiation covering the Sbk2 gene. Exons are presented by the various red peaks, and the splice junctions are presented by the red arcs. The *Rattus norvegicus* Sbk2 transcript (ENSRNOT00000058956.3) is depicted below the sashimi plot, with the white and red rectangles representing the protein-coding sequences and untranslated regions (UTRs), respectively. **B**, Changes in Sbk2 expression (transcripts per million [TPM]) during a full cycle of iAM-1 cell differentiation (quasi-Poisson regression phase I, red line, n=4) and dedifferentiation (quasi-Poisson regression phase II, green line, n=4). (*Continued*)

of NRAMs for Sbk2 and cardiac Mybpc3 (myosin-binding protein C) indicated that the localization of Sbk2 extends beyond the area in which Mybpc3 is localized (Figure S10).[29] Collectively, these findings indicate that Sbk2 is localized in very close proximity to the myosin heads in the sarcomeric A-band of rats and humans.

Targeted Knockdown of Sbk2 Expression Demonstrates a Role in Sarcomere Formation and Maintenance

To study the biological role of Sbk2, we employed 2 LVVs encoding, in addition to *Aequorea victoria* eGFP (enhanced green fluorescent protein), different RnSbk2-specific shRNAs (Figure S11A). Isogenic LVVs coding for rat Nxk2-5 (RnNkx2-5)- or Ppluc (firefly luciferase)-specific shRNAs were included as positive and negative vector controls, respectively. The role of Sbk2 during cardiomyogenic differentiation was studied by transducing iAMs with the shRNA-encoding LVVs shortly after doxycycline removal. At d9 of cardiomyogenic differentiation, the relative expression level of Sbk2 in cells transduced with either of the four shRNA-encoding LVVs was determined by RT-qPCR (Figure 6A) and compared with that of proliferating iAMs, NRAMs and neonatal rat ventricular myocytes. In accordance with the transcriptome analysis, Sbk2 expression of iAMs significantly increased (≈9-fold, *n*=6) during cardiomyogenic differentiation. Also, Sbk2 expression was higher in NRAMs compared with neonatal rat ventricular myocytes, which is consistent with RT-qPCR and Western blot results of heart tissue (Figure 4C and 4D; Figure S6A through S6C), but lower than in (proliferating) iAMs. Furthermore, RnSbk2-specific shRNA No. 1, which targeted the coding sequence of Sbk2, caused a 54% reduction of Sbk2 expression (relative quantity, 0.46 [95% CI, 0.36–0.54], n=6), whereas RnSbk2-specific shRNA No. 2, which targeted the 3′ untranslated region of Sbk2, reduced Sbk2 expression with 78% (relative quantity, 0.22 [95% CI, 0.01–0.44], n=6). The RnNkx2-5-specific shRNA increased Sbk2 expression (relative quantity, 2.34 [95% CI, 2.07′2.61], n=6), while the Ppluc-specific shRNA did not significantly alter the Sbk2 mRNA level (Figure 6A). Western blot analysis corroborated the RT-qPCR results by showing an increase in Sbk2 expression during iAM differentiation and a repressive effect of the RnSbk2-specific shRNAs but not of the control shRNAs on the Sbk2 protein level in differentiated iAMs (Figure 6B). As expected, the RnNkx2-5-specific shRNA strongly reduced the Nxk2-5 protein level in iAMs at day 9 of differentiation in contrast to the other three shRNAs (Figure 6B). Importantly, at similar LVV doses (based on eGFP expression levels), none of the shRNAs substantially affected the expression of other sarcomeric proteins such as Actn2 and cardiac α-actin (Actc1; Figure 6B).

The biological effects of targeted Sbk2 knockdown were studied by immunostaining of iAMs fixed at day 9 of cardiomyogenic differentiation with antibodies directed against Sbk2 and Actn2 (Figure 6C through 6F). For these experiments, nonsaturating vector doses were used to prevent overdosing of individual cells and to guarantee the presence of nontransduced (ie, $eGFP^{-}$) control cells in each culture. Diferentiated iAMs expressing the Ppluc-specific shRNA showed nonoverlapping striated staining patterns for Actn2 and Sbk2 (Figure 6C) indicative of the presence of highly organized sarcomeres and consistent with the immunohistochemical results presented in Figure 5 and in Figure S6 and S8. In the cells transduced with the LVV encoding the Nkx2-5-specific shRNA, the sarcomeric organization was lost as evinced by scattered staining patterns of Actn2 and Sbk2 (Figure 6D), while the absolute levels of these proteins were not affected (Figure 6B). In line with the RT-qPCR and Western blot results, both Sbk2-specific shRNAs caused an absolute decrease in the Sbk2 staining intensity and a disorganized Actn2 staining pattern reminiscent of premyofibrils (Figure 6E and 6F). Immunocytochemistry of primary neonatal rat cardiomyocytes, once more confirmed that Sbk2 is highly enriched in NRAMs (Figure S13A and S13B) and that the targeted knockdown of Sbk2 in these cells results in similar structural abnormalities as observed in iAMs (Figure S13C through S13F). Overexpression of epitope-tagged RnSbk2 (HA~RnSbk2) but not *Escherichia coli* β-galactosidase (HA~βGal) could prevent the sarcomeric breakdown caused by the RnSbk2-specific shRNAs (Results in the Supplemental Material, Figures S14 and S15). The disruptive effect of SBK2 downregulation on sarcomeres was confirmed in a human atrial model by showing that targeted knockdown of HsSBK2 in hiAMs inhibited sarcomere formation/maintenance (Results in the Supplemental Material and Figure S16). Additionally, neither knockdown nor overexpression of Sbk2 affected the electrophysiological properties of differentiated

Figure 4 Continued. C and **D**, Analysis of the Sbk2 expression in neonatal rats by Western blotting (**C**) and RT-qPCR (**D**) in various cardiac and noncardiac tissues. Lamin A/C (Lmna) served as loading control for the Western blot. RT-qPCR data of RnSbk2 were normalized using transcripts of 2 housekeeping genes (ie, Rn18S and Rpl4). Data are presented as mean relative quantities (RQs) and corresponding SD, n=3. X means not expressed. **E** through **M**, Immunohistological double stainings of Sbk2 and the Z-line marker desmin (Des) in neonatal rat heart (**E**, **H**, **K**) and neonatal rat liver (**G**) sections. The section shown in (**F**) was incubated with secondary antibodies only. (**I** and **L**) show enlargements of the randomly selected atrial and ventricular regions of interest from (**K**) used to produce representative sarcomeric line scans (**J** and **M**). Ao indicates aorta; AoV, aortic valve(s); CoA, coronary artery; Ect, ectopic expression of Sbk2 in HEK293T cells (using the vector depicted in Figure S10B); LA, left atrium; Liv, liver; Lng, lung; LV, left ventricle; RA, right atrium; RV, right ventricle; Ske, skeletal muscle; and Spl, spleen.

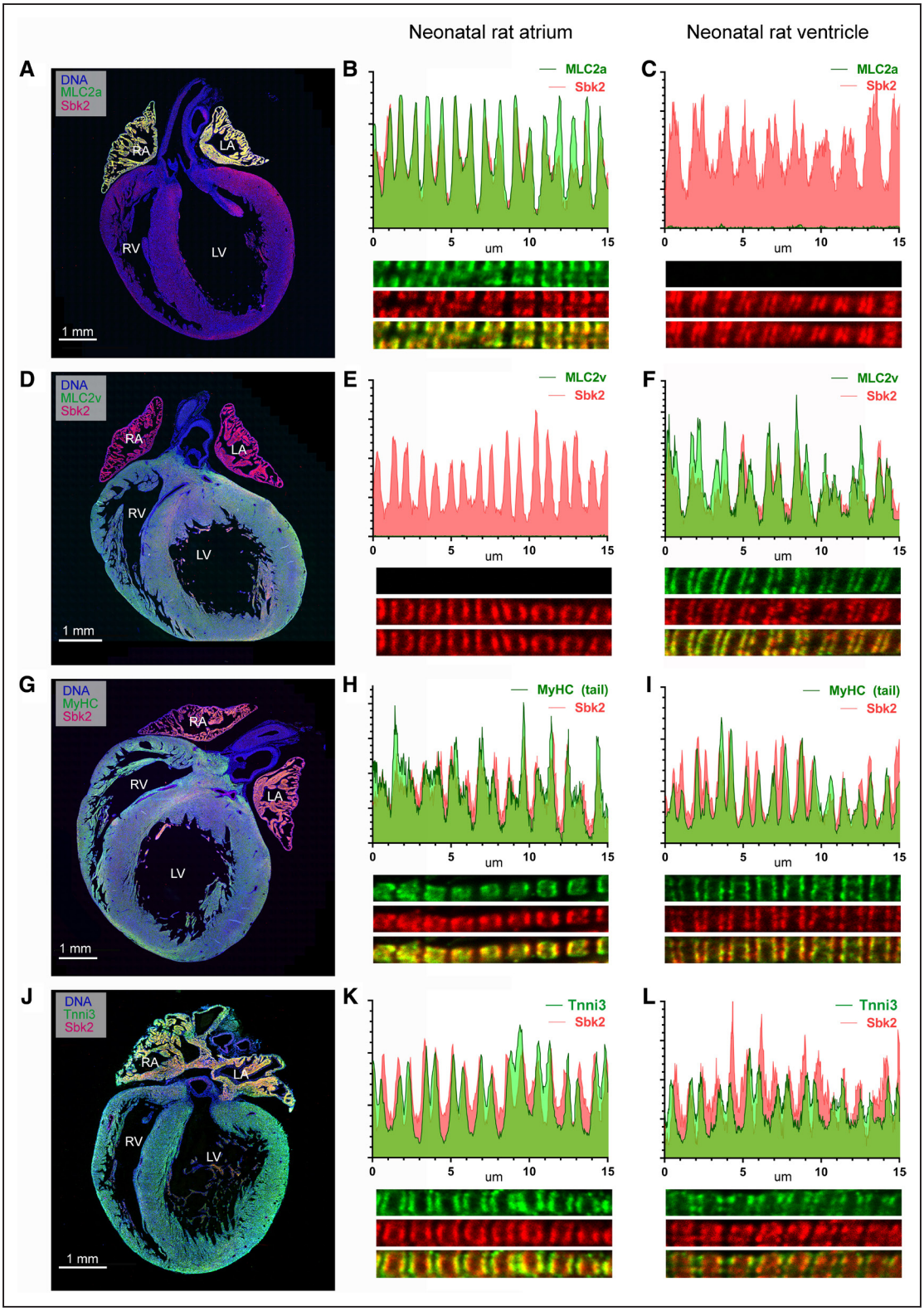

Figure 5. Sbk2 (SH3 domain binding kinase family member 2) is localized near the myosin heads in the sarcomeric A-band of neonatal rat hearts.

A–**L**, Immunohistochemical double stainings of coronal sections of neonatal rat hearts (**A**, **D**, **G**, **J**) and their corresponding line scans (**B**, **C**, **E**, **F**, **H**, **I**, **K**, **L**) of Sbk2 and the MLC2a (atrial marker myosin light chain 2a; **A**–**C**), MLC2v (ventricular marker myosin light chain 2v; **D**–**F**), tail region of MyHC (myosin heavy chain II protein; **G**–**I**), and Tnni3 (cardiac troponin I; **J**–**L**). LA indicates left atrium; LV, left ventricle; RA, right atrium; and RV, right ventricle.

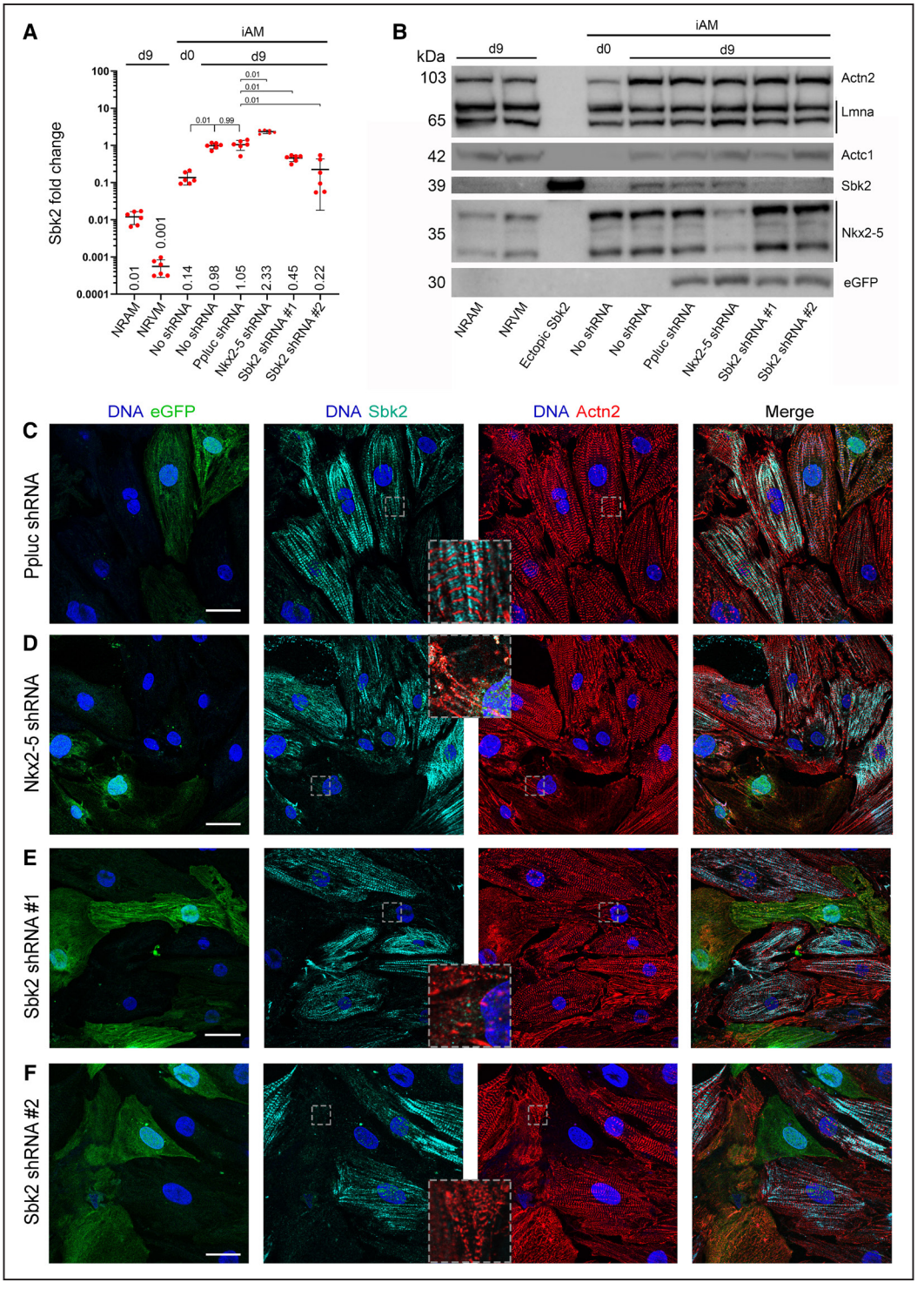

Figure 6. Targeted knockdown of Sbk2 (SH3 domain binding kinase family member 2) demonstrates a role in sarcomeric formation in conditionally immortalized neonatal rat atrial myocytes (iAMs).

A and **B**, Analysis of Sbk2 expression in untransduced primary cardiomyocytes (ie, NRAMs and neonatal rat ventricular myocytes [NRVMs]), proliferating iAMs (d0) and differentiated iAMs (d9) and in differentiated iAMs following lentiviral shRNA-mediated knockdown of Ppluc (negative control), RnNkx2-5 (positive control) or RnSbk2 (2 different vectors) by reverse transcription-quantitative polymerase chain reaction (RT-qPCR; **A**) and Western blotting (**B**). RT-qPCR data of RnSbk2 (rat Sbk2; **A**) were normalized using transcripts of 2 housekeeping genes (ie, Rn18S and Rpl4). Data are presented as mean relative quantities (RQs) and corresponding SD, n=6. Statistics were done using a one-way ANOVA test with Tukey post hoc correction. Lamin A/C (Lmna) served as loading control for the Western blot and eGFP was detected to confirm that similar doses of each of the shRNA-encoding lentiviral vectors (LVV) were used for targeted knockdown of gene expression. The specificity of the vectors was checked by staining for Actn2 (cardiac α-actinin), Actc1 (cardiac α-actin), Sbk2, and Nkx2-5. **C**–**F**, Immunocytochemical double stainings for Sbk2 and Actn2 (cardiac α-actinin) of iAMs transduced with LVVs encoding eGFP and shRNAs targeting Ppluc (**C**), RnNkx2-5 (**D**), or RnSbk2 (**E** and **F**). Scale bar, 25 μm.

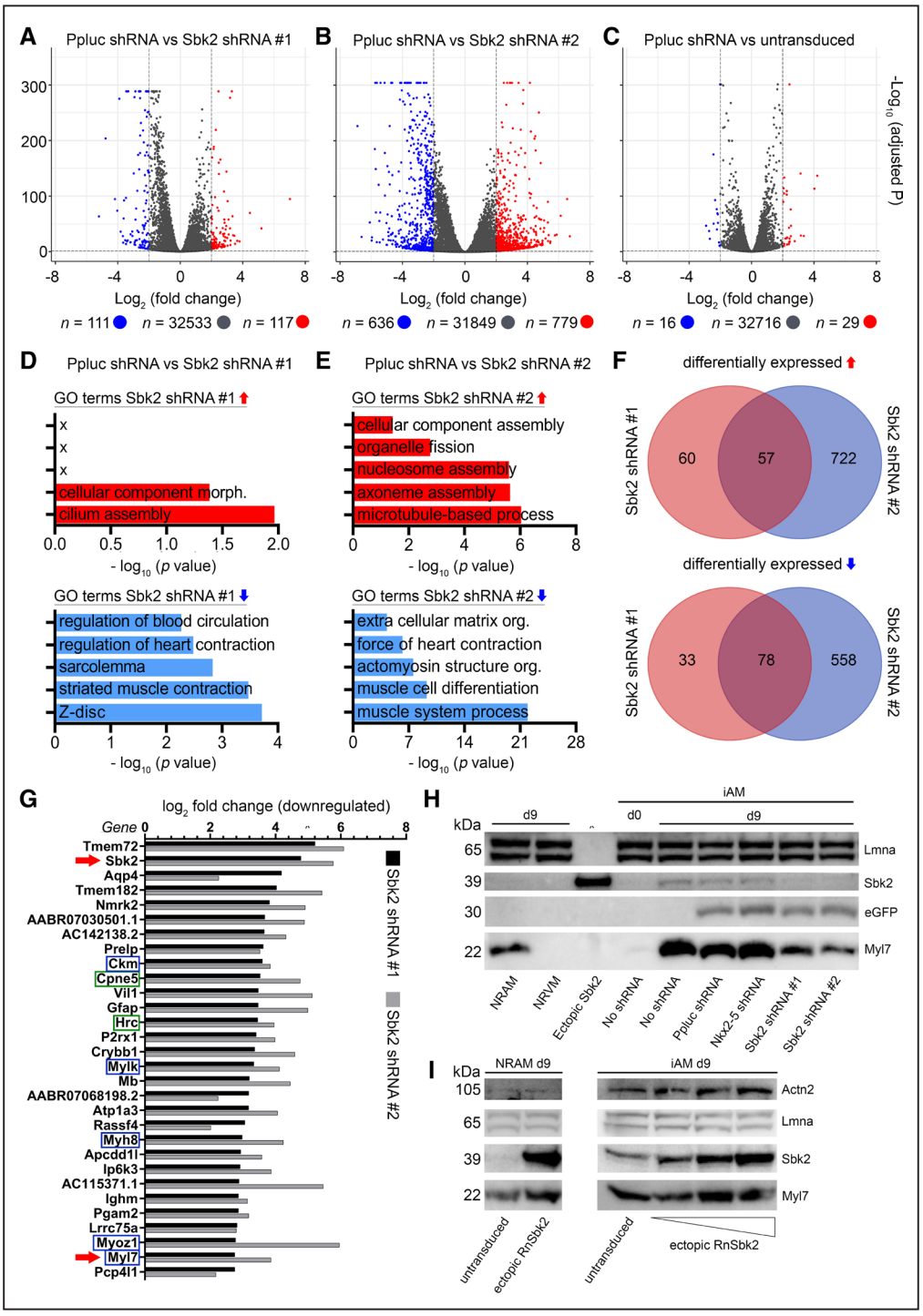

Figure 7. Knockdown transcriptome of conditionally immortalized neonatal rat atrial myocytes (iAM-1s) identifies Sbk2 (SH3 domain binding kinase family member 2) as regulator of Myl7 expression.

A–**C**, Volcano plots comparing gene expression between differentiated iAM-1 cells expressing the Ppluc-specific shRNA and differentiated iAM-1 cells expressing RnSbk2 shRNA No. 1 (**A**), rat Sbk2 (RnSbk2) shRNA No. 2 (**B**) or no shRNA (untransduced; **C**). **D** and **E**, Gene ontology (GO) terms associated with the differentially expressed genes between the Ppluc shRNA samples and the RnSbk2 shRNA No. 1 (**D**) or RnSbk2 shRNA No. 2 (**E**) samples including their statistical significance as represented by the corrected *P* values (Benjamini-Hochberg method). For nonabbreviated GO terms, see Table S9. **F**, Venn diagram of the differentially expressed genes presented in (**A**) and (**B**). **G**, The top 30 downregulated genes (sorted from high to low, based on RnSbk2 shRNA No. 1) that are differentially expressed between the Ppluc shRNA and both RnSbk2-specific shRNAs (n=78). Sarcomeric and Ca^{2+}-handling proteins are indicated by blue and green boxes, respectively. **H**, Myl7, Sbk2, and eGFP expression in untransduced primary rat cardiomyocytes (ie, neonatal rat atrial myocytes [NRAMs] and neonatal rat ventricular myocytes [NRVMs]), proliferating iAMs (d0) and differentiated iAMs (d9) and in differentiated iAMs following lentiviral shRNA-mediated knockdown of Ppluc, RnNkx2-5 or RnSbk2 (2 different vectors) by Western blotting. (**I**) Myl7 and Actn2 (cardiac α-actinin) expression in untransduced and ectopically RnSbk2 expressing cardiomyocytes (ie, NRAMs and iAMs). Lamin A/C (Lmna) served as loading control for the Western blots.

iAM monolayers (Figure S17). Taken together, these knockdown experiments implicate an important role of RnSbk2 and HsSBK2 in atrial sarcomere formation/maintenance in rats and humans, respectively.

Knockdown of Sbk2 Expression in iAM-1 Cells Strongly Reduces Sarcomeric mRNA and Protein Levels

To gain mechanistic insight into the disruptive effect of SBK2 downregulation on sarcomeres, iAM-1 cells were transduced with LVVs encoding Ppluc- or RnSbk2-specific shRNAs at day 1 of differentiation followed by transcriptome analysis of mRNA samples harvested at d9. mRNA from fully differentiated untransduced iAM-1 cells was included as reference. As shown in Figure 7C and Figure S18, the transcriptomes of untransduced iAM-1 cells and iAM-1 cells expressing the Ppluc-specific shRNA were very similar with only few genes being differentially expressed (Table S9). In contrast, both RnSbk2-specific shRNAs greatly altered the transcriptome of iAM-1 cells (Figure 7A and 7B). In comparison with the Ppluc-specific shRNA, Sbk2 shRNA No. 2 gave rise to more differentially expressed genes than Sbk2 shRNA No. 1, most likely due to the higher knockdown efficiency of Sbk2 shRNA No. 2 (Figures 6A, 7G, and 7H). Nevertheless, the GO terms associated with the differentially up- and downregulated genes (Figure 7D and 7E) showed the involvement of similar biological processes for both RnSbk2-specific shRNAs. Knockdown of Sbk2 resulted in downregulation of genes involved in muscle development and contraction, which is in line with the observed immunocytological phenotype (Figure 6C through 6F). Venn diagrams of the differentially expressed genes for both Sbk2-specific shRNAs (Figure 7F) showed that 78 of the 111 genes (ie, 70.3%) downregulated by Sbk2 shRNA No. 1 were also downregulated by Sbk2 shRNA No. 2. Several of the overlapping downregulated genes, including Myh6, Myh7, Myh8, Myl7, Mylk, and Myoz1 encode sarcomeric proteins. Of these genes, Mylk, Myh8, Myoz1, and Myl7 were among the 30 genes showing the highest decrease in expression level upon Sbk2 knockdown (Figure 7G) The consequences of Sbk2 knockdown on sarcomeric gene expression were confirmed at the protein level by mass spectrometry (Figure S19 and Table S10) and additionally validated by Western blotting for the Myl7-encoded Mlc2a protein (Figure 7H). Furthermore, Western blotting showed in both NRAMs and iAMs that ectopic expression of RnSbk2 results in an RnSbk2 dose-dependent increase of Mlc2a, while Actn2 levels were not affected by knockdown (Figure 6B; Figure S19D and S19G) or overexpression (Figure 7I) of RnSbk2.

As a final experiment, possible interaction partners of RnSbk2 in differentiated iAM-1 cells overexpressing epitope-tagged versions of RnSbk2 or *Oplophorus gracilirostris* enhanced NanoLuc luciferase (as negative control bait) were identified by co-immunoprecipitation and mass spectrometry (Results in the Supplemental Material, Figure S20, and Table S10). These experiments identified proteins with diverse cellular functions (translation, intracellular trafficking, cytoskeletal organization, chromatin modification, sarcomere formation) as possible interaction partners of Sbk2.

DISCUSSION

In this study, we exploited the unique ability of conditionally immortalized neonatal rat atrial cardiomyocytes to switch, in a doxycycline-dependent manner, between a noncontractile proliferative phenotype and a nonproliferative contractile phenotype for studying the transcriptional changes during cardiomyocyte differentiation and dedifferentiation.[21] Transcriptome profiling of iAM-1 cells confirmed the phenotypic plasticity of these cells. In the presence of doxycycline, iAM-1 cells showed generally high expression of genes involved in cell proliferation and mostly low expression of genes with a specific function in (cardio)myocytes, which were both largely reversed after doxycycline removal. By mining the gene expression data of iAM-1 cells for cardiac-enriched transcripts of low abundance, we identified 28 genes with a likely but yet uninvestigated role during cardiomyocyte differentiation. Of these genes, Sbk2 was selected for further investigation as it displayed the largest fold changes in expression level during phenotypic switching and has not been studied before. Our results show that the Sbk2 gene, which codes for a highly conserved serine/threonine protein kinase, is selectively expressed in striated muscle tissue with dominant expression in both atria. Detailed immunohistochemical analyses of rat hearts and human atrial appendages revealed that the Sbk2 protein is localized in very close proximity to the myosin heads of cardiac sarcomeres. Lentiviral shRNA-mediated suppression of Sbk2/SBK2 expression during (h)iAM differentiation disturbed (proper) sarcomere formation. The changes in transcriptome and proteome induced by Sbk2 knockdown in differentiated iAM-1 cells and the Sbk2-binding proteins identified by co-immunoprecipitation indicate involvement of Sbk2 in different processes including mRNA translation, intracellular trafficking, cytoskeletal organization, and sarcomere formation.

Animal in vivo models have been instrumental in expanding our understanding of heart morphogenesis, cardiac cell differentiation, and cardiac disease. Although in vivo models usually have greater physiological relevance, in vitro models are generally less costly and easier to work with allowing the assessment of gene function in a highly controllable, systematic and reproducible manner by pharmaceutical or genetic interventions.[30] Moreover, the use of animals for biomedical research is facing growing public disapproval.[9] These arguments have provided a strong incentive for the replacement of animal in vivo models by more animal-friendly in vitro models based on animal or human (i)PSCs and cell lines with preserved cell type-specific functions.

Motivated by the difficulty to generate large numbers of fully functional AMs from (i)PSCs, our research group developed the iAM,[21] and more recently, the hiAM cell lines[22] for both basic and translational cardiac research. Since the gene expression profile of proliferating (h)iAMs is controlled by an oncoprotein (ie, simian virus 40 large T antigen), whose synthesis is induced by the presence of doxycycline, it is distinct from that of cardiac mesodermal or progenitor cells. As a consequence, the cardiomyogenic differentiation of iAMs in the absence of doxycycline does not fully reflect the natural course of events occurring during embryonic heart development.[8,31] Because doxycycline is present in a relatively low concentration (100 ng/mL) only during the proliferation of (h)iAMs and since the inhibitory effect of doxycycline on mitochondrial respiration has been shown to be reversible, doxycycline is unlikely to (negatively) affect (h)iAM differentiation (Discussion in the Supplemental Material).[32,33] Furthermore, upon doxycycline removal, iAM-1 cells show robust upregulation of the expression of a multitude of genes engaged in cardiomyocyte differentiation and function (Figures 2 and 3; Figure S2; and Table S7), including genes encoding regulators of cardiomyogenesis (receptors, ligands, adaptors, transcriptional [co-]activators, transcriptional [co-]repressors), sarcomeric components (eg, Tcap, Tnni3) and proteins involved in cardiac action potential generation and propagation (eg, Gja1, Gjc1), Ca^{2+} handling (eg, Cmya5, Trdn), and energy metabolism (eg, Cox8b, Prkag2). This, together with the ease with which iAMs can be multiplied, differentiated, genetically modified and functionally tested, makes them a highly attractive model for the identification and characterization of factors with a thus far unexplored role in (atrial) cardiomyocyte formation and activity.

Interestingly, of the 28 cardiac-enriched low-abundance transcripts whose expression increased ≥2-fold during iAM-1 cell differentiation and decreased again ≥2-fold during subsequent dediffferentiation, >3-quarters have not been studied in the context of the heart. Among these genes, Sbk2, Doc2g,[34] and Klhl38[35] stand out for being preferentially expressed in atrial, cardiac, and striated muscle tissue, respectively. The Sbk2 gene codes for a protein kinase, which is one of the largest protein groups in eukaryotes. In humans, >500 protein kinase genes have been identified corresponding to almost 2% of the protein-coding genes in the human genome.[36] Protein kinases modulate the activity of proteins in a graded or binary fashion through the addition of phosphate from ATP mainly to the hydroxyl groups of serine, threonine, and tyrosine residues. Phosphorylation is the most frequent (reversible) posttranslational modification of proteins and controls a large variety of cellular processes including DNA replication and cell division, transcription and translation, cell metabolism, signal transduction, and cytoskeletal organization. A recent study estimates the number of phosphoproteins in the human proteome at 13 000.[37] Abnormal protein phosphorylation has been linked to numerous human diseases[38] including myocardial hypertrophy,[39] heart failure,[40] and atrial fibrillation.[41] Phylogenetic analysis primarily on the basis of the amino acid sequences of the kinase domains has led to the identification of 8 protein kinase families, namely AGC, Atypical, CAMK, CK1, CMGC, STE, TK, and TKL.[28] Sbk2 does not group to one of these protein kinase families but is part of a novel protein kinase family designated NKF1 (new kinase family 1),[36] which further comprises Sbk1 and Sbk3 (also known as Sgk110). These kinases are most related to the CMGC family of protein kinases, which includes amongst others the CDKs (cyclin-dependent kinases), GSKs (glycogen synthase kinases), and MAPKs (mitogen-activated protein kinases).[36] The best studied NKF1 member is Sbk1, which is not expressed in iAMs, while SBK1 expression in hiAMs is very low and declining during cardiomyogenic differentiation. A previous study has shown that Sbk1 is a widely expressed cytosolic protein with oncogenic potential.[42] Moreover, the *Drosophila* orthologue of Sbk1 has been shown to play a role in long-term brain memory.[43] The closest relative to Sbk2 is Sbk3. The Sbk2 and Sbk3 genes are located with a few kb distance of each other highlighting their common origin. Interestingly, Sbk3 is also one of the 28 genes encoding cardiac-enriched low-abundance transcripts showing a ≥2-fold higher expression in differentiated iAM-1 cells than in their proliferating counterparts. In addition, Sbk3 transcripts have a similar spatiotemporal distribution pattern as Sbk2 transcripts, being enriched in the atria and showing a trend of being upregulated during the transition from neonate to adult (Figure S21). Interestingly, RNA-Seq of the left and right atria of human fetal and adult hearts showed HsSBK2 expression to be much higher in fetal hearts, while human SBK3 transcript levels were somewhat higher in adult hearts.[44] In iAM-1 cells, Sbk2 knockdown did not induce Sbk1 expression and suppressed Sbk3 expression (≈1.8- and 4.9-fold by RnSbk2 shRNA No. 1 and No. 2, respectively, Table S9), demonstrating that the Sbk2 knockdown studies were not confounded by compensatory effects of other NKF1 members. Lastly, experiments in NRAMs revealed no significant effects of doxycycline on Sbk2 or Sbk3 mRNA levels (Figure S22), while repeated switching of hiAMs between proliferative and differentiated states did not reduce their cardiomyogenic ability,[22] demonstrating the validity of our experimental models.

In recent years, protein kinases have been shown to regulate the assembly, maintenance and contractility of sarcomeres and a well-kept balance between the activity of protein kinases and phosphatases acting on sarcomeric components is important for proper heart function.[45–48] Most of the sarcomeric protein kinases and phosphatases localize at specific positions along the myofilaments especially in the Z-discs and M-bands but also in between these structures. The importance of protein kinases for maintaining sarcomere integrity is nicely illustrated by a recent study in *Caenorhabditis elegans* in

which individual knockdown of the expression of 34 different kinase genes caused disorganization/tearing of sarcomeres.[49] No substrates have been identified for any of the NKF1 members. However, based on the subcellular localization of Sbk2 and sarcomere-disrupting effects of Sbk2/SBK2 knockdown, proteins directly or indirectly involved in cardiac sarcomerogenesis are likely interaction partners of Sbk2. Remarkably, among the protein species most frequently co-immunoprecipitated with RnSbk2 from lysates of differentiated iAM-1 cells were, besides sarcomeric components, many polypeptides involved in intracellular trafficking, cytoskeletal organization, and protein translation. This raises the interesting but as of yet purely hypothetical possibility that Sbk2 is a regulator of the recently discovered process of localized sarcomeric protein translation.[50] If so, knockdown of Sbk2 could inhibit translation of sarcomeric mRNAs, which could accelerate degradation of (some of) these transcripts[51] and thereby have profound effects on AM structure and function. Such a scenario could also explain the extensive alterations in differentiated iAM-1 transcriptome and proteome following RNAi-mediated Sbk2 downregulation. Future studies focusing on Sbk2's interaction partners including dedicated mass spectrometry-based phosphoproteomics together with investigations of the functional consequences of Sbk2-mediated phosphorylation events will be required to unravel the pathways by which Sbk2 regulates sarcomere formation and maintenance.

In conclusion, in this study, we have demonstrated the utility of recently generated conditionally immortalized NRAMs as an easy-to-use model to identify and characterize new factors involved in (atrial) cardiomyogenesis. By employing RNA-Seq, the dynamic changes in gene expression accompanying the doxycycline-dependent transition of iAMs from a proliferative to a differentiated state and vice versa were investigated. This led to the discovery of a multitude of genes with likely but yet uninvestigated roles in (atrial) cardiomyocyte differentiation including the serine/threonine protein kinase-encoding Sbk2 gene. Detailed analysis of the Sbk2 protein showed that it is preferentially expressed in AMs, localizes to the A-band of cardiac sarcomeres and is an important regulator of atrial sarcomere formation/maintenance.

ARTICLE INFORMATION

Received March 31, 2021; revision received March 8, 2022; accepted May 10, 2022.

Affiliations

Laboratory of Experimental Cardiology, Department of Cardiology (P.R.R.v.G., J.Z., J.L., S.O.D., C.I.B., T.D.C., M.J.S., D.E.A., D.A.P., A.A.F.d.V.), Department of Biomedical Data Sciences, Medical Statistics Section (R.T.), and Sequencing Analysis Support Core, Department of Biomedical Data Sciences (H.M.), Leiden University Medical Center, the Netherlands. Central Laboratory, Longgang District People's Hospital of Shenzhen & The Third Affiliated Hospital of The Chinese University of Hong Kong, China (J.L.). Biomolecular Mass Spectrometry and Proteomics, Bijvoet Center for Biomolecular Research and Utrecht Institute for Pharmaceutical Sciences, University of Utrecht, the Netherlands (H.P., A.J.R.H.). Netherlands Proteomics Centre, the Netherlands (H.P., A.J.R.H.).

Sources of Funding

This research was funded by the More Knowledge with Fewer Animals (MKMD) project with number 114022503 (to A.A.F. de Vries), which is (partly) financed by the Netherlands Organisation for Health Research and Development (ZonMw) and the Dutch Society for the Replacement of Animal Testing (dsRAT). Additional support was provided by the Leiden Regenerative Medicine Platform Holding (LRMPH project 8212/41235 to A.A.F. de Vries).

Disclosures

None.

Supplemental Materials

Extended Methods, Supplementary Results and Supplementary Discussion
Figures S1–S22
Tables S1–S10
References 52–58

REFERENCES

1. Akerberg BN, Pu WT. Genetic and epigenetic control of heart development. *Cold Spring Harb Perspect Biol.* 2020;12:a036756. doi: 10.1101/cshperspect.a036756
2. Williams K, Carson J, Lo C. Genetics of congenital heart disease. *Biomolecules.* 2019;9:E879. doi: 10.3390/biom9120879
3. Meganathan K, Sotiriadou I, Natarajan K, Hescheler J, Sachinidis A. Signaling molecules, transcription growth factors and other regulators revealed from in-vivo and in-vitro models for the regulation of cardiac development. *Int J Cardiol.* 2015;183:117–128. doi: 10.1016/j.ijcard.2015.01.049
4. Kain KH, Miller JW, Jones-Paris CR, Thomason RT, Lewis JD, Bader DM, Barnett JV, Zijlstra A. The chick embryo as an expanding experimental model for cancer and cardiovascular research. *Dev Dyn.* 2014;243:216–228. doi: 10.1002/dvdy.24093
5. James JF, Hewett TE, Robbins J. Cardiac physiology in transgenic mice. *Circ Res.* 1998;82:407–415. doi: 10.1161/01.res.82.4.407
6. Piazza N, Wessells RJ. Drosophila models of cardiac disease. *Prog Mol Biol Transl Sci.* 2011;100:155–210. doi: 10.1016/B978-0-12-384878-9.00005-4
7. Bakkers J. Zebrafish as a model to study cardiac development and human cardiac disease. *Cardiovasc Res.* 2011;91:279–288. doi: 10.1093/cvr/cvr098
8. DeLaughter DM, Bick AG, Wakimoto H, McKean D, Gorham JM, Kathiriya IS, Hinson JT, Homsy J, Gray J, Pu W, et al. Single-cell resolution of temporal gene expression during heart development. *Dev Cell.* 2016;39:480–490. doi: 10.1016/j.devcel.2016.10.001
9. Wadman M. A trans-Atlantic transparency gap on animal experiments. *Science.* 2017;357:119–120. doi: 10.1126/science.357.6347.119
10. Protze SI, Lee JH, Keller GM. Human pluripotent stem cell-derived cardiovascular cells: from developmental biology to therapeutic applications. *Cell Stem Cell.* 2019;25:311–327. doi: 10.1016/j.stem.2019.07.010
11. Cyganek L, Tiburcy M, Sekeres K, Gerstenberg K, Bohnenberger H, Lenz C, Henze S, Stauske M, Salinas G, Zimmermann WH, et al. Deep phenotyping of human induced pluripotent stem cell-derived atrial and ventricular cardiomyocytes. *JCI Insight.* 2018;3:99941. doi: 10.1172/jci.insight.99941
12. van den Berg CW, Okawa S, de Sousa Lopes SMC, van Iperen L, Passier R, Braam SR, Tertoolen LG, del Sol A, Davis RP, Mummery CL. Transcriptome of human foetal heart compared with cardiomyocytes from pluripotent stem cells. *Development.* 2015;142:3231–3238. doi: 10.1242/dev.123810
13. Biendarra-Tiegs SM, Li X, Ye D, Brandt EB, Ackerman MJ, Nelson TJ. Single-cell RNA-sequencing and optical electrophysiology of human induced pluripotent stem cell-derived cardiomyocytes reveal discordance between cardiac subtype-associated gene expression patterns and electrophysiological phenotypes. *Stem Cells Dev.* 2019;28:659–673. doi: 10.1089/scd.2019.0030
14. Dillies MA, Rau A, Aubert J, Hennequet-Antier C, Jeanmougin M, Servant N, Keime C, Marot G, Castel D, Estelle J, et al; French StatOmique Consortium. A comprehensive evaluation of normalization methods for Illumina high-throughput RNA sequencing data analysis. *Brief Bioinform.* 2013;14:671–683. doi: 10.1093/bib/bbs046
15. van Bakel H, Nislow C, Blencowe BJ, Hughes TR. Most "dark matter" transcripts are associated with known genes. *PLOS Biol.* 2010;8:e1000371. doi: 10.1371/journal.pbio.1000371
16. Kalsotra A, Cooper TA. Functional consequences of developmentally regulated alternative splicing. *Nat Rev Genet.* 2011;12:715–729. doi: 10.1038/nrg3052

17. Tarazona S, García-Alcalde F, Dopazo J, Ferrer A, Conesa A. Differential expression in RNA-seq: a matter of depth. *Genome Res*. 2011;21:2213–2223. doi: 10.1101/gr.124321.111
18. Jiang L, Schlesinger F, Davis CA, Zhang Y, Li R, Salit M, Gingeras TR, Oliver B. Synthetic spike-in standards for RNA-seq experiments. *Genome Res*. 2011;21:1543–1551. doi: 10.1101/gr.121095.111
19. Curion F, Handel AE, Attar M, Gallone G, Bowden R, Cader MZ, Clark MB. Targeted RNA sequencing enhances gene expression profiling of ultra-low input samples. *RNA Biol*. 2020;17:1741–1753. doi: 10.1080/15476286.2020.1777768
20. Halvardson J, Zaghlool A, Feuk L. Exome RNA sequencing reveals rare and novel alternative transcripts. *Nucleic Acids Res*. 2013;41:e6. doi: 10.1093/nar/gks816
21. Liu J, Volkers L, Jangsangthong W, Bart CI, Engels MC, Zhou G, Schalij MJ, Ypey DL, Pijnappels DA, de Vries AAF. Generation and primary characterization of iAM-1, a versatile new line of conditionally immortalized atrial myocytes with preserved cardiomyogenic differentiation capacity. *Cardiovasc Res*. 2018;114:1848–1859. doi: 10.1093/cvr/cvy134
22. Harlaar N, Dekker SO, Zhang J, Snabel RR, Veldkamp MW, Verkerk AO, Fabres CC, Schwach V, Lerink LJS, Rivaud MR, et al. Conditional immortalization of human atrial myocytes for the generation of in vitro models of atrial fibrillation. *Nat Biomed Eng*. 2022;6:389–402. doi: 10.1038/s41551-021-00827-5
23. Robinson MD, McCarthy DJ, Smyth GK. edgeR: a Bioconductor package for differential expression analysis of digital gene expression data. *Bioinformatics*. 2010;26:139–140. doi: 10.1093/bioinformatics/btp616
24. Love MI, Huber W, Anders S. Moderated estimation of fold change and dispersion for RNA-seq data with DESeq2. *Genome Biol*. 2014;15:550. doi: 10.1186/s13059-014-0550-8
25. Yu Y, Fuscoe JC, Zhao C, Guo C, Jia M, Qing T, Bannon DI, Lancashire L, Bao W, Du T, et al. A rat RNA-Seq transcriptomic BodyMap across 11 organs and 4 developmental stages. *Nat Commun*. 2014;5:3230. doi: 10.1038/ncomms4230
26. Huang da W, Sherman BT, Lempicki RA. Systematic and integrative analysis of large gene lists using DAVID bioinformatics resources. *Nat Protoc*. 2009;4:44–57. doi: 10.1038/nprot.2008.211
27. Cui S, Ji T, Li J, Cheng J, Qiu J. What if we ignore the random effects when analyzing RNA-seq data in a multifactor experiment. *Stat Appl Genet Mol Biol*. 2016;15:87–105. doi: 10.1515/sagmb-2015-0011
28. Hanks SK, Hunter T. Protein kinases 6. The eukaryotic protein kinase superfamily: kinase (catalytic) domain structure and classification. *FASEB J*. 1995;9:576–596.
29. Craig R, Lee KH, Mun JY, Torre I, Luther PK. Structure, sarcomeric organization, and thin filament binding of cardiac myosin-binding protein-C. *Pflugers Arch*. 2014;466:425–431. doi: 10.1007/s00424-013-1426-6
30. van Gorp PRR, Trines SA, Pijnappels DA, de Vries AAF. Multicellular in vitro models of cardiac arrhythmias: focus on atrial fibrillation. *Front Cardiovasc Med*. 2020;7:43. doi: 10.3389/fcvm.2020.00043
31. Paige SL, Plonowska K, Xu A, Wu SM. Molecular regulation of cardiomyocyte differentiation. *Circ Res*. 2015;116:341–353. doi: 10.1161/CIRCRESAHA.116.302752
32. Protasoni M, Kroon AM, Taanman JW. Mitochondria as oncotarget: a comparison between the tetracycline analogs doxycycline and COL-3. *Oncotarget*. 2018;9:33818–33831. doi: 10.18632/oncotarget.26107
33. Luger AL, Sauer B, Lorenz NI, Engel AL, Braun Y, Voss M, Harter PN, Steinbach JP, Ronellenfitsch MW. Doxycycline impairs mitochondrial function and protects human glioma cells from hypoxia-induced cell death: implications of using tet-inducible systems. *Int J Mol Sci*. 2018;19:E1504. doi: 10.3390/ijms19051504
34. Fukuda M, Mikoshiba K. Doc2gamma, a third isoform of double C2 protein, lacking calcium-dependent phospholipid binding activity. *Biochem Biophys Res Commun*. 2000;276:626–632. doi: 10.1006/bbrc.2000.3520
35. Ehrlich KC, Baribault C, Ehrlich M. Epigenetics of muscle- and brain-specific expression of KLHL family genes. *Int J Mol Sci*. 2020;21:E8394. doi: 10.3390/ijms21218394
36. Manning G, Whyte DB, Martinez R, Hunter T, Sudarsanam S. The protein kinase complement of the human genome. *Science*. 2002;298:1912–1934. doi: 10.1126/science.1075762
37. Vlastaridis P, Kyriakidou P, Chaliotis A, Van de Peer Y, Oliver SG, Amoutzias GD. Estimating the total number of phosphoproteins and phosphorylation sites in eukaryotic proteomes. *Gigascience*. 2017;6:1–11. doi: 10.1093/gigascience/giw015
38. Cohen P. The role of protein phosphorylation in human health and disease. The Sir Hans Krebs Medal Lecture. *Eur J Biochem*. 2001;268:5001–5010. doi: 10.1046/j.0014-2956.2001.02473.x
39. Yan K, Wang K, Li P. The role of post-translational modifications in cardiac hypertrophy. *J Cell Mol Med*. 2019;23:3795–3807. doi: 10.1111/jcmm.14330
40. Pfleger J, Gresham K, Koch WJ. G protein-coupled receptor kinases as therapeutic targets in the heart. *Nat Rev Cardiol*. 2019;16:612–622. doi: 10.1038/s41569-019-0220-3
41. Heijman J, Ghezelbash S, Wehrens XH, Dobrev D. Serine/Threonine phosphatases in atrial fibrillation. *J Mol Cell Cardiol*. 2017;103:110–120. doi: 10.1016/j.yjmcc.2016.12.009
42. Wang P, Guo J, Wang F, Shi T, Ma D. Human SBK1 is dysregulated in multiple cancers and promotes survival of ovary cancer SK-OV-3 cells. *Mol Biol Rep*. 2011;38:3551–3559. doi: 10.1007/s11033-010-0465-8
43. Lee PT, Lin G, Lin WW, Diao F, White BH, Bellen HJ. A kinase-dependent feedforward loop affects CREBB stability and long term memory formation. *Elife*. 2018;7:e33007. doi: 10.7554/eLife.33007
44. van Ouwerkerk AF, Bosada FM, van Duijvenboden K, Hill MC, Montefiori LE, Scholman KT, Liu J, de Vries AAF, Boukens BJ, Ellinor PT, et al. Identification of atrial fibrillation associated genes and functional non-coding variants. *Nat Commun*. 2019;10:4755. doi: 10.1038/s41467-019-12721-5
45. Peng Y, Gregorich ZR, Valeja SG, Zhang H, Cai W, Chen YC, Guner H, Chen AJ, Schwahn DJ, Hacker TA, et al. Top-down proteomics reveals concerted reductions in myofilament and Z-disc protein phosphorylation after acute myocardial infarction. *Mol Cell Proteomics*. 2014;13:2752–2764. doi: 10.1074/mcp.M114.040675
46. Fuller SJ, Osborne SA, Leonard SJ, Hardyman MA, Vaniotis G, Allen BG, Sugden PH, Clerk A. Cardiac protein kinases: the cardiomyocyte kinome and differential kinase expression in human failing hearts. *Cardiovasc Res*. 2015;108:87–98. doi: 10.1093/cvr/cvv210
47. Reimann L, Wiese H, Leber Y, Schwäble AN, Fricke AL, Rohland A, Knapp B, Peikert CD, Drepper F, van der Ven PF, et al. Myofibrillar Z-discs Are a Protein Phosphorylation Hot Spot with Protein Kinase C (PKCα) Modulating Protein Dynamics. *Mol Cell Proteomics*. 2017;16:346–367. doi: 10.1074/mcp.M116.065425
48. Westfall MV. Contribution of post-translational phosphorylation to sarcomere-linked cardiomyopathy phenotypes. *Front Physiol*. 2016;7:407. doi: 10.3389/fphys.2016.00407
49. Lehmann S, Bass JJ, Szewczyk NJ. Knockdown of the C. elegans kinome identifies kinases required for normal protein homeostasis, mitochondrial network structure, and sarcomere structure in muscle. *Cell Commun Signal*. 2013;11:71. doi: 10.1186/1478-811X-11-71
50. Lewis YE, Moskovitz A, Mutlak M, Heineke J, Caspi LH, Kehat I. Localization of transcripts, translation, and degradation for spatiotemporal sarcomere maintenance. *J Mol Cell Cardiol*. 2018;116:16–28. doi: 10.1016/j.yjmcc.2018.01.012
51. Morris C, Cluet D, Ricci EP. Ribosome dynamics and mRNA turnover, a complex relationship under constant cellular scrutiny. *Wiley Interdiscip Rev RNA*. 2021;12:e1658. doi: 10.1002/wrna.1658
52. Livingstone CD, Barton GJ. Protein sequence alignments: a strategy for the hierarchical analysis of residue conservation. *Comput Appl Biosci*. 1993;9:745–756. doi: 10.1093/bioinformatics/9.6.745
53. Ge X. iDEP web application for RNA-Seq data analysis. *Methods Mol Biol*. 2021;2284:417–443. doi: 10.1007/978-1-0716-1307-8_22
54. Tyanova S, Temu T, Sinitcyn P, Carlson A, Hein MY, Geiger T, Mann M, Cox J. The Perseus computational platform for comprehensive analysis of (prote)omics data. *Nat Methods*. 2016;13:731–740. doi: 10.1038/nmeth.3901
55. Bindea G, Mlecnik B, Hackl H, Charoentong P, Tosolini M, Kirilovsky A, Fridman WH, Pagès F, Trajanoski Z, Galon J. ClueGO: a Cytoscape plug-in to decipher functionally grouped gene ontology and pathway annotation networks. *Bioinformatics*. 2009;25:1091–1093. doi: 10.1093/bioinformatics/btp101
56. Allen PS, Dell'Italia LJ, Esvelt M, Conte ML, Cadillac JM, Myers DD. Cardiovascular research. In: Suckow MA, Hankenson FC, Wilson RP, Foley PL, eds. *The Laboratory Rat*. 3rd ed. Elsevier; 2020:927–965.
57. Moullan N, Mouchiroud L, Wang X, Ryu D, Williams EG, Mottis A, Jovaisaite V, Frochaux MV, Quiros PM, Deplancke B, et al. Tetracyclines disturb mitochondrial function across eukaryotic models: a call for caution in biomedical research. *Cell Rep*. 2015;10:1681–1691. doi: 10.1016/j.celrep.2015.02.034
58. Valderrábano M. Influence of anisotropic conduction properties in the propagation of the cardiac action potential. *Prog Biophys Mol Biol*. 2007;94:144–168. doi: 10.1016/j.pbiomolbio.2007.03.014